Journal of the American Heart Association

ORIGINAL RESEARCH

Left Atrial Remodeling Identification and Catheter Ablation Outcomes With ^{18}F-Fluorodeoxyglucose Positron Emission Tomography in Persistent Atrial Fibrillation

Tristan Raoult, MD; Bernhard L. Gerber, MD, PhD; Quentin Garnir, MD; Christophe Scavée, MD; Varnavas Varnavas, MD, PhD; Aurélien Wauters, MD, PhD; Damien Gruson, MD, PhD; Eric Nellessen, MD; Michel Hesse, PhD; Christophe Beauloye, MD, PhD; Véronique Roelants, MD, PhD; Sébastien Marchandise, MD, PhD

BACKGROUND: Left atrial structural remodeling contributes to the persistence of atrial fibrillation (AF) and influences the outcomes of catheter ablation (CA). We investigated the usefulness of ^{18}F-fluorodeoxyglucose-positron emission tomography in detecting low atrial glucose uptake (LGU) as a potential marker of fibrosis and its predictive value for CA success in persistent AF.

METHODS: Thirty-six patients without diabetes with persistent AF scheduled for CA underwent nicotinic acid-stimulated ^{18}F-fluorodeoxyglucose-positron emission tomography to assess global and segmental LGU before CA. LGU was compared with low voltage areas on electroanatomical mapping, left atrial volume index via echocardiography, and late gadolinium enhancement from cardiac magnetic resonance imaging as indicators of fibrosis. Patients were followed for up to 24 months post CA to assess AF recurrence.

RESULTS: Global LGU extent was 16.8% (7.6–42.6) and correlated with left atrial volume index (R^2=0.20, P=0.039) and low voltage area during AF and right atrial pacing (R^2=0.54 and R^2=0.35 respectively, both P<0.001). Multivariable analysis showed that LGU significantly predicted moderate/severe low voltage area remodeling (P<0.001) with an area under the curve of 0.78 (95% CI, 0.58–0.97), independent of clinical and imaging parameters. AF recurred in 50% of patients. LGU >17%, but not late gadolinium enhancement, predicted AF recurrence (P=0.026; AUC, 0.67 [95% CI, 0.48–0.86]).

CONCLUSIONS: Nicotinic acid-enhanced ^{18}F-fluorodeoxyglucose-positron emission tomography LGU extent reflects fibrosis by low voltage areas and predicts AF recurrence after CA in patients with persistent AF. This suggests that it could serve as a noninvasive tool for assessing atrial fibrosis and remodeling in atrial cardiomyopathy due to persistent AF.

Key Words: ^{18}F-FDG-PET ■ atrial cardiomyopathy ■ glucose metabolism ■ left atrial structural remodeling ■ low glucose uptake extent ■ persistent atrial fibrillation

Catheter ablation (CA) with pulmonary vein isolation (PVI) has gained widespread acceptance as the fundamental therapeutic approach for symptomatic paroxysmal atrial fibrillation (AF).[1–3] However, the management of persistent AF (peAF) or long-standing AF presents a more intricate challenge, marked by less favorable outcomes and a heightened recurrence rate following isolated PVI.[4,5] Consequently, efforts persist

Correspondence to: Sébastien Marchandise, MD, PhD, Division of Cardiology, Department of Cardiovascular Diseases, Cliniques Universitaires St. Luc UCLouvain, Av Hippocrate 10/2806, B-1200 Woluwe St. Lambert, Belgium. Email: sebastien.marchandise@saintluc.uclouvain.be

This article was sent to Kevin F. Kwaku, MD, PhD, Associate Editor, for review by expert referees, editorial decision, and final disposition.

Supplemental Material is available at https://www.ahajournals.org/doi/suppl/10.1161/JAHA.124.041491

For Sources of Funding and Disclosures, see page 14.

JAHA is available at: www.ahajournals.org/journal/jaha

CLINICAL PERSPECTIVE

What Is New?

- Nicotinic acid–enhanced ^{18}F-fluorodeoxyglucose-positron emission tomography (PET) imaging accurately identifies low-voltage areas and fibrosis/structural remodeling of the left atrium in patients with persistent atrial fibrillation.
- Among noninvasive modalities, low atrial glucose uptake measured by ^{18}F-fluorodeoxyglucose-PET in the atrial walls demonstrates the highest diagnostic accuracy for predicting the extent of low voltage areas; low atrial glucose uptake identified by PET imaging is a strong, independent predictor of atrial fibrillation recurrence after catheter ablation.

What Are the Clinical Implications?

- ^{18}F-fluorodeoxyglucose-PET provides a novel, noninvasive tool to characterize atrial fibrosis and remodeling, potentially guiding personalized ablation strategies in persistent atrial fibrillation.
- PET-based assessment of atrial glucose metabolism may improve patient selection and inform risk stratification for atrial fibrillation recurrence after ablation.
- Further research is needed to validate the clinical value of noninvasive ^{18}F-fluorodeoxyglucose-PET imaging in larger populations and to strengthen its role in understanding the pathophysiology of atrial cardiomyopathy.

Nonstandard Abbreviations and Acronyms

CA	catheter ablation
EAVM	electroanatomical voltage mapping
^{18}F-FDG	^{18}F-fluorodeoxyglucose
LAVI	left atrial volume indexed
LGE	late gadolinium enhancement
LGU	low glucose uptake
LVA	low voltage area
SUV	standardized uptake value

to develop supplementary strategies to enhance the efficacy of AF ablation. Left atrial (LA) structural remodeling is a hallmark of atrial cardiomyopathy in peAF, which is intricately linked to increased fibrosis, thereby prognosticating poorer outcomes.[6–8] Therefore, in patients with peAF and LA cardiomyopathy, the identification and assessment of the AF substrate and specifically atrial fibrosis have high clinical value, as the CA strategy is progressively transitioning toward a customized approach, targeting these fibrotic areas as the underlying substrate for arrhythmia.[9–12] Low voltage area (LVA), identified by electroanatomical voltage mapping (EAVM), has emerged as the gold standard for identifying such atrial fibrosis and guiding ablation strategies.[9–11] However, due to its invasive nature, this procedure can be conducted only at the time of CA. Therefore, there is a growing interest in noninvasive cardiac imaging techniques such as transthoracic echocardiography,[13,14] and 3-dimensional (3D) gated late gadolinium-enhanced whole-heart navigator cardiac magnetic resonance (LGE-CMR) for identifying atrial fibrosis[15,16] and predicting CA success rate.[17] Nevertheless, ambiguous results have been reported when comparing LGE-CMR and EAVM in localizing LA fibrosis. The recent DECAAF II (Efficacy of Delayed Enhancement MRI [Magnetic Resonance Imaging]-Guided Ablation vs Conventional Catheter Ablation of Atrial Fibrillation) trial did not meet expectations with no demonstrable improvement in outcomes for CMR-guided ablation, confirming the difficulty in developing a tailored approach based on identifying the arrhythmic substrate with noninvasive imaging tools.[18–20]

We recently presented findings indicating that nicotinic acid-stimulated ^{18}F-fluorodeoxyglucose (^{18}F-FDG) uptake enables high-quality imaging of atrial metabolism in peAF.[21] Building on this, we hypothesize that akin to the left ventricle (LV), under such metabolic conditions, atrial myocardial FDG uptake identifies the viability of atrial myocytes. Consequently, area exhibiting metabolic defects and low atrial glucose uptake (LGU) could identify the absence of atrial myocardial viability and the presence of atrial fibrosis.

Hence, the current study aims to assess the potential usefulness of ^{18}F-FDG positron emission tomography (PET) to identify LA fibrosis in peAF. To achieve this, we conducted a comprehensive multimodal comparison of FDG-PET LGU with other established markers of atrial scar, specifically LVA extent assessed by EAVM in patients with peAF undergoing CA. In addition, we sought to investigate whether LGU ^{18}F-FDG uptake could also serve predict the success of the CA procedures in these patients.

METHODS

The data that support the findings of this study are available from the corresponding author upon reasonable request.

Detailed methods are provided in Data S1.

Study Design and Population

This single-center study was approved by our institutional review board (2018/17OCT/389. TRIATLON;

Eudract reference 2019-001813-17A), and all participants provided written informed consent. The study protocols and methods were reported before.[21] Briefly, adult patients referred to our facility for an initial CA procedure between January 2020 and September 2022 were eligible for inclusion, if they presented peAF, without history of prior AF ablation treatment. Exclusion criteria were diabetes; hyperthyroidism; renal failure (glomerular filtration rate<30 mL/m^2); infiltrative, hypertrophic, or other cardiomyopathies; severe valvular disease; and preoperative transesophageal echocardiography-determined LA appendage thrombus. The study protocol consisted of atrial cardiac magnetic resonance imaging, transthoracic echocardiography and a nicotinic acid enhanced atrial ^{18}F-FDG PET scan before EAVM and CA procedure. All imaging was performed while patients were in AF.

Cardiac MR

CMR was acquired using a 3T system and consisted of a 3D magnetic resonance contrast-enhanced angiographic image of the LA acquired after 0.1 mmol/kg Gd-DTPA injection, cine short-axis and long axis to evaluate LV and right ventricular and LA end-diastolic and end-systolic volumes and ejection fractions. Twenty minutes after contrast injection, evaluation of LA fibrosis was performed using a free-breathing navigator gated 3D whole heart late gadolinium sequence with a high resolution (1.5×1.5×1.5 mm).

Echocardiography

Preintervention, a comprehensive 2-dimensional transthoracic echocardiography was acquired to measure LV volumes, ejection fraction, diastolic function (mitral E/e′ ratio), LA volumes indexed to body surface area (LAVI) and LA ejection fraction according to guidelines. Reservoir global peak atrial longitudinal strain was computed using LV end-diastole as a zero-strain point. The LA stiffness index was calculated as E/e′ divided by global peak atrial longitudinal strain.[14]

Atrial ^{18}F-FDG PET Imaging

^{18}F-FDG PET/computed tomography (CT) was performed after overnight fasting and administration of a nicotinic acid derivative (acipimox 250 mg) to maximize myocardial glucose uptake as described previously.[21] A 10-minute partial volume and spillover corrected atrial image was acquired 90 minutes after injection of 300 MBq of ^{18}F-FDG. Atrial glucose standardized uptake value (SUV) was computed for each voxel by taking account for the injected ^{18}F tracer activity per patient body weight (MBq/kg) and decay correction.

Electroanatomical Mapping and Catheter Ablation Procedure

LA endocardial EAVM was performed with CARTO3 system at the time of CA. Bipolar peak-to-peak voltage amplitudes were recorded while the patient was in AF, then after electrical cardioversion during right atrial pacing at 100 beats per minute. After voltage mapping, all patients benefited from point-by-point radiofrequency energy in an antral circumferential ablation pattern around each PV pair according to the CLOSE protocol (enclosing the PV with contiguous and optimized radiofrequency lesions)[22] with complete PVI and supplementary line ablation at the physician's discretion.

Image Processing and Fibrosis Quantification

DICOM PET-CT, LGE-CMR, and raw 3D data of the atria from the CARTO3 system were imported into Slicer-3D software. Point cloud measurements of bipolar voltages were orthogonally projected and interpolated on the model's surfaces to recreate 3D voltage maps. (Figure 1). Then PET-CT, LGE-CMR, and EAVM were visually aligned with magnetic resonance contrast-enhanced angiographic images, and the LA wall was segmented by delineating the epicardial and endocardial contours of the atria on axial slices. 3D models for PET-CT, LGE-CMR, magnetic resonance contrast-enhanced angiography, and EAVM were generated and coregistered using an iterative closest point algorithm (12 degrees of freedom, allowing for deformation and scaling). Before quantification, we manually excluded PVs and the mitral valve using the dynamic modeler tool within Slicer3D. (Figure 1). LVAs were identified when bipolar peak-to-peak voltage amplitude was <0.30 mV during AF and 0.50 mV during right atrial pacing. The global LVA extent was calculated as a percentage of LA surface as previously described,[21] and LVA extent >15% was considered as moderate or important.[21] The global LA voltage was calculated as the mean of the bipolar peak-to-peak voltage amplitudes measured in the whole atria, excluding the PVs and the mitral valve. Fibrosis by LGE-CMR was evaluated using as reference 2 SDs above the average intensity of the mean blood signal intensity enhancement. AF-LGE was categorized into Utah stages I through IV, corresponding to atrial LGE of 0% to 10%, 10% to 20%, 20% to 40%, and >40%, respectively.[17] LGU was quantified as the ratio of the LA surface displaying an SUV below a threshold defined as the mean±5 SDs of the blood SUV. LVA, LGU extent, voltage, and SUV measurements were conducted in the anterior, inferior, and posterior segments.[2] In this case, values were indexed to the corresponding surface area.

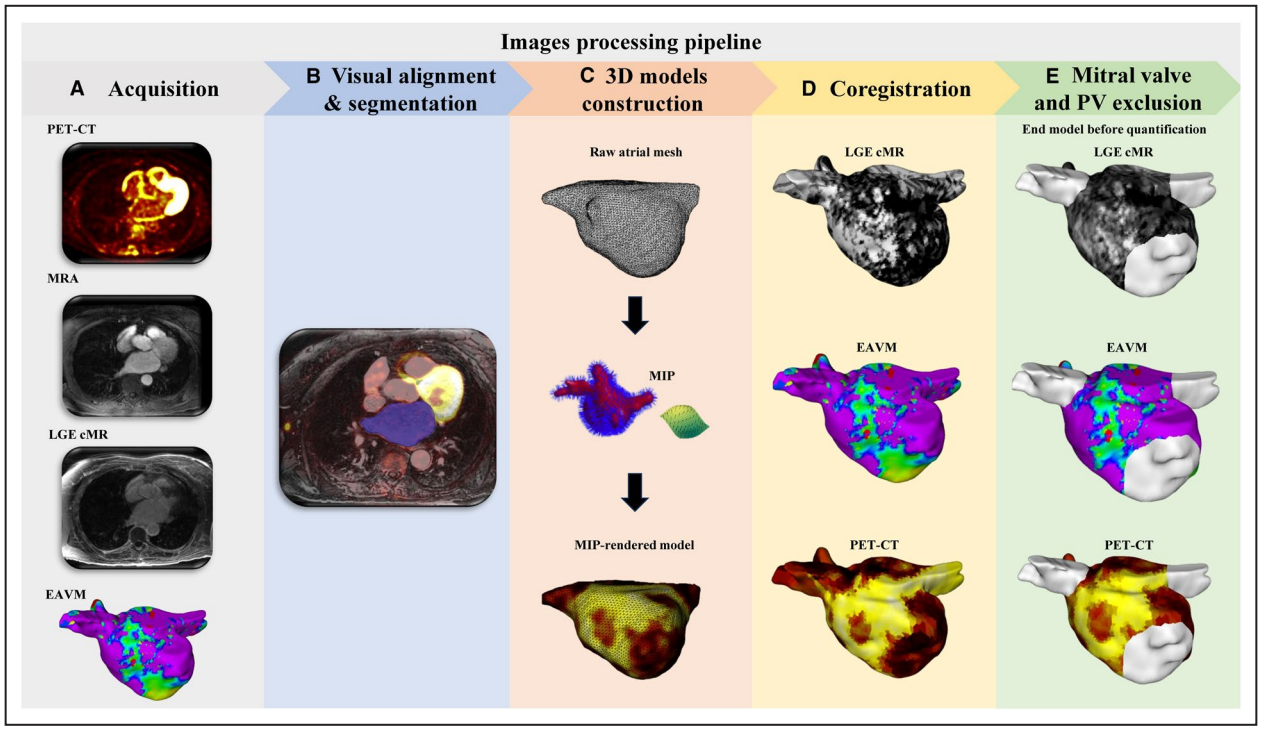

Figure 1. Workflow of the acquisition, alignment, segmentation, and postprocessing of left atrial CMRI LGE, left atrial EAVM and left atrial ^{18}F-FDG-PET images.

A, Images were acquired during AF before the ablation procedure (CMR—^{18}F-FDG) and were at first visually aligned with CMR angiographic images. **B**, The segmentations of the LA in DE-CMR and PET were reformated as 3D models. **C**, A maximum-intensity projection of the values inside the atrial wall was used to overlay the models. **D**, All models, including the EAVM, were then coregistered with a 3D model reconstructed from magnetic resonance angiography, using an iterative closest point algorithm (12 degrees of freedom, including deformation and scaling). This allows direct comparison by visual inspection. **E**, LGE fibrosis extent (CMR), LVA extent (EAVM), and LGU extent (^{18}F-FDG PET) were identified and quantified after excluding the mitral valve and pulmonary vein volumes. ^{18}F-FDG indicates ^{18}F-fluorodeoxyglucose; 3D, 3-dimensional; AF, atrial fibrillation; CT, computed tomography; DE, delayed enhancement; EAVM electroanatomical voltage mapping; LA, left atrium; LGE CMR, late gadolinium enhancement cardiac magnetic resonance; LGU, low glucose uptake; LVA, low voltage area; MIP, maximum intensity projection; MRA, magnetic resonance contrast-enhanced angiographic; PET, positron emission tomography; and PV, pulmonary vein.

Statistical Analysis

$P<0.05$ was considered indicative of a statistically significant difference. Continuous values were assessed for normality and expressed as the mean±1 SD or the median with interquartile range depending on their distribution. Categorical variables were expressed as counts and percentages. To compare groups, 2-sided *t* test or the Mann–Whitney *U* test were used as appropriate for continuous variables, and categorical data were compared using chi-square or Fisher's exact tests as appropriate. Analysis of variance was used to normalize for confounding variables. Multivariable linear regression models were used to compare patient and imaging modalities characteristics with severity of LVA extent parameters. receiver operating characteristic models and logistic regression models were used to compare several thresholds with continuous variables. Area under the curve (AUC) was compared with Delong test. The relationship between the different imaging modalities were evaluated through linear regression analysis and the Pearson correlation coefficient. Receiver operating characteristic models and logistic regression models were used to predict LVA extent. Patients were separated into 2 groups according to the median LGU extent value (LGU-Group I with LGU≤median value and LGU-Group II with LGU>median value). Survival free from AF recurrence after CA was analyzed using Kaplan–Meier and multivariable Cox survival analysis.

RESULTS

Study Participants and Baseline Characteristics

This study included 38 patients with peAF. Two patients were excluded, one due to the inability to obtain images caused by PET scanner failure and the other due to poor image quality resulting from an issue with tracer injection. Patient baseline characteristics are summarized in Table 1.

AF persisted for >6 months in 53% of subjects, with a median of AF duration of 150 days. The median

Table 1. Characteristics of the Study Population

	All patients (n=36)	LGU≤17% (n=18)	LGU>17% (n=18)	*P* value*
Clinical parameters				
Age, y	64.3±8.7	62.9±8.4	65.5±8.8	0.205
Sex (male)	27 (75)	14 (77.7)	13 (72.2)	0.341
Persistent AF duration, d	200 (180–285)	109 (105–190)	180 (150–365)	0.056
Estimated glomerular filtration rate, mL/min	74±22	73±12	69±23	0.285
CHA_2DSVAS_2C	2 (1–3)	2 (1–3)	2 (1–3)	0.5
Cohorts for Heart and Aging Research in Genomic Epidemiology-AF	12.4±1.1	11.8±0.9	12.6±1.2	0.106
Antiarrhythmic drugs	16 (44.4)	9 (50)	7 (38.8)	
Cardiovascular risk factors				
Active tobacco use	11 (30.5)	6 (33.3)	5 (27.8)	0.362
Coronary artery disease	7 (18.42)	2 (11.1)	5 (27.8)	0.224
Hypertension	14 (36.8)	4 (22.2)	9 (50)	0.169
Hypercholesterolemia	16 (42.1)	6 (33.3)	11 (61.1)	0.046
Diabetes	0 (0.0)	0 (0.0)	0 (0.0)	NA
Echocardiographic parameters				
LVEF, %	58.2±9.4	61.4±7.7	55.2±10.1	0.029
LAVI, mL/m^2	59.9±18.3	57.0±19.6	62.9±16.9	0.178
E/e′	8.8±3.9	7.3±2.1	10.2±4.6	0.15
LA diameter, mm	47.2±5.21	45.6±5.2	48.7±4.9	0.044
LA stiffness index	1.2±0.8	0.9±0.3	1.4±0.9	0.014
Global peak atrial longitudinal strain, %	9.0±3.4	9.5±3.8	8.6±3.1	0.213
Positron emission tomography parameters				
LA mean SUV global	3.6 (3.2–4.7)	4.7 (4.3–5.9)	3.2 (2.9–3.6)	<0.001
LA mean SUV posterior	3.5 (2.8–4.8)	4.8 (3.6–5.4)	2.8 (2.7–3.4)	<0.001
LA mean SUV inferior	3.5 (2.8–4.5)	4.5 (4.0–5.8)	3.0 (2.7–3.4)	<0.001
LA mean SUV anterior	4.5 (3.6–5.8)	5.8 (4.5–7.0)	3.6 (3.2–4.3)	<0.001
LA global LGU (%)	16.8 (7.6–42.6)	7.6 (3.7–10.2)	44.5 (24.9–56.6)	<0.001
LA posterior LGU (%)	26.3 (5.5–52.7)	5.5 (2.7–14.2)	53.9 (41.2–73.4)	<0.001
LA inferior LGU (%)	21.3 (7.3–43.9)	7.3 (1.4–12.4)	44.5 (37.9–60.2)	<0.001
LA anterior LGU (%)	9.3 (1.9–27.7)	1.9 (0.3–5.8)	24.0 (12.9–36.3)	<0.001
Cardiac magnetic resonance parameters				
LV mass indexed, g/m^2	55.4±13.2	53.9±17.2	62.2±20.8	0.097
LVEDVi, mL/m^2	77.5±20.16	77.9±17.7	80.8±22.3	0.339
LVEF, %	50.1±8.4	52.1±7.3	50.1±9.1	0.227
RVEDVi, mL/m^2	75.5±15.2	76.6±14.8	74.2±14.1	0.307
RVEF, %	51.1±8.2	51.4±7.1	52.1±9.1	0.371
LAVI, mL/m^2	77.0±24.1	71.9±26.7	81.4±20.5	0.133
Fibrosis, %	10.0 (5.6–17.0)	8.9 (6.8–16.9)	11.5 (4.7–15.3)	0.349

Data are presented as mean±SD, number (percentage), or median (interquartile range). *P* value* compares group LGU≤17% and LGU>17%. AF indicates atrial fibrillation; EDVi, end diastolic volume indexed; EF, ejection fraction; LA, left atrium; LAVI, left atrium volume indexed; LGU, low glucose uptake; LV, left ventricle; NA, not applicable; RV, right ventricle; and SUV, standardized uptake value.

CHA2DS2-VASc score was 2, and 11% of patients had a history of stroke or systemic thromboembolism.

Imaging Results

The mean LAVI was 59.9±18.3 ml, the mean GPALS was 9%, and mean LA stiffness index was 1.2±0.8. The average atrial LGE extent was 12.28%±9.47% (range 1%–45%). Nine patients (25%) were classified as Utah stage I, 20 (56%) as Utah stage II, 6 (19%) as Utah stage 3, and only 1 as Utah stage 4. No indications of infiltrative diseases such as amyloidosis or sarcoidosis was found in the study population. Patients with peAF exhibited variable global

Table 2. Procedural Characteristics During AF

	All patients	LGU≤17%	LGU >17%	*P* value*
Global LVA extent, %	6.3 (0.5– 25.4)	0.9 (0.2– 6.3)	19.5 (7.6– 34.1)	<0.001
Posterior LVA extent, %	2.5 (0.3– 21.4)	0.2 (0.1– 1.8)	15.2 (2.8– 32.5)	0.010
Inferior LVA extent, %	2.0 (0.1– 12.5)	0.2 (0.1– 2.0)	11.6 (5.9– 29.6)	0.003
Anterior LVA extent, %	3.3 (0.4– 30.9)	0.7 (0.1– 3.4)	24.9 (2.9– 37.6)	0.012
Global LA voltage, mV	0.71 (0.51– 1.07)	0.94 (0.67– 1.39)	0.58 (0.42– 0.68)	0.002
Voltage posterior LA, mV	0.64 (0.45– 0.95)	0.88 (0.64– 1.20)	0.51 (0.43– 0.67)	0.010
Voltage inferior LA, mV	0.72 (0.53– 0.93)	0.91 (0.71– 1.17)	0.54 (0.48– 0.67)	0.031
Voltage anterior LA, mV	0.67 (0.43– 1.09)	1.09 (0.67– 1.47)	0.53 (0.43– 0.74)	0.007
AF rhythm during electroanatomical voltage mapping	36 (100)	18 (100)	18 (100)	NA
Pulmonary vein isolation	36 (100)	18 (100)	18 (100)	NA
Cavotricuspid isthmus ablation	5 (13.9)	3 (16.6)	2 (11.1)	0.685
Posterior wall isolation	6 (16.6)	2 (11.1)	4 (22.2)	0.357
Mitral isthmus	3 (8.3)	1 (5.5)	2 (11.1)	0.534
Complex atrial fractionated electrogram	2 (5.5)	1 (5.5)	1 (5.5)	0.971
Procedural time, min	164±36	159±37	163±35	0.765
Irradiation, mGy/cm^2	2994±1519	2869±1242	3075±1661	0.665

Data are presented as mean±SD, number (percentage) or median (interquartile range). AF indicates atrial fibrillation; LA, left atrial; LGU, low glucose uptake; LVA, low voltage area; and NA, not applicable. *P* value* compares group LGU≤17% and LGU>17%.

LGU extent, with a median of 16.8% (7.6–42.6), and LGU extent represented 26.3% (5.5–52.7) in the posterior segment, 21.3% (7.3–43.9) in the inferior segment, and 9.3% (1.9–27.7) in the anterior segment of the LA. Based on median global LGU extent, patients were divided into 2 groups: Group I (mild LGU extent with LGU≤17%), and Group II (moderate or important LGU extent with LGU>17%). Compared with patients with global LGU ≤17%, patients with higher LGU had higher blood pressure (*P*=0.041), had a longer median duration of persistent AF (*P*=0.056), slightly lower LV ejection fraction (*P*=0.029), and higher LA diameter (*P*=0.044) or LA stiffness index (*P*=0.014). No significant differences were observed in LGE fibrosis between the 2 groups.

Procedural and EAVM Characteristics

The procedural characteristics are summarized in Table 2.

EAVM were successfully reproduced during AF in all patients before CA procedure, using 2072±874 acquired points and revealing a median global LVA extent of 6.3% (0.5–25.4) and median global LA voltage of 0.68 mV (0.55–1.01). Most patients, 31 (86%), presented with LVA.

Global LVA extent was markedly higher (19.3% versus 3.5%, *P*<0.001), and global voltage was lower (0.58 mV versus 0.94 mV, *P*=0.002) in patients with elevated extent of global LGU. This difference was also present in the segmental analysis. EAVM data acquired during right atrial pacing are detailed in Data S2, Table S1, and

Figure 2. Segmented 3D ^{18}F-FDG uptake map relationship with 3D EAVM acquired during AF ablation procedure in PA and AP views.

The color gradient of the LVA maps indicates endocardial electrogram amplitude from pink (>0.3 mV in AF) to red (at <0.1 mV). The color gradient of the LGU maps indicates ^{18}F-FDG standardized uptake value amplitude from dark/brown (LGU area) to yellow (without LGU area). **A**, Illustration of a patient showing a homogenous distribution of the tracer without LGU extent in the LA wall. Color 3D EAVM shows electrically normal atrial tissue without LVA. **B**, Illustration of a LA with moderate remodeling, displaying a heterogeneous tracer distribution indicating LGU area in the posterior and inferior segments of the LA, particularly around the left inferior PV and right inferior PV ostia. LGU is also evident in the anteroseptal region of the LA. Color 3D EAVM in the PA and AP views show abnormal atrial tissue with LVA in the corresponding region. **C**, Illustration of a LA with extensive remodeling. Heterogeneity of the tracer distribution is more pronounced with significant LGU in the LA's posteroinferior, anterior, and anteroseptal regions, corresponding on EAVM to abnormal atrial tissue with LVA. ^{18}F-FDG indicates ^{18}F-fluorodeoxyglucose; 3D, 3-dimensional; AF, atrial fibrillation; AP, anteroposterior view; EAVM, electroanatomical voltage mapping; LA, left atrium; LGU, low glucose uptake; LVA, low voltage area; mV, millivolts; PA, posteroanterior view; PV, pulmonary vein; and SUV, standardized uptake value.

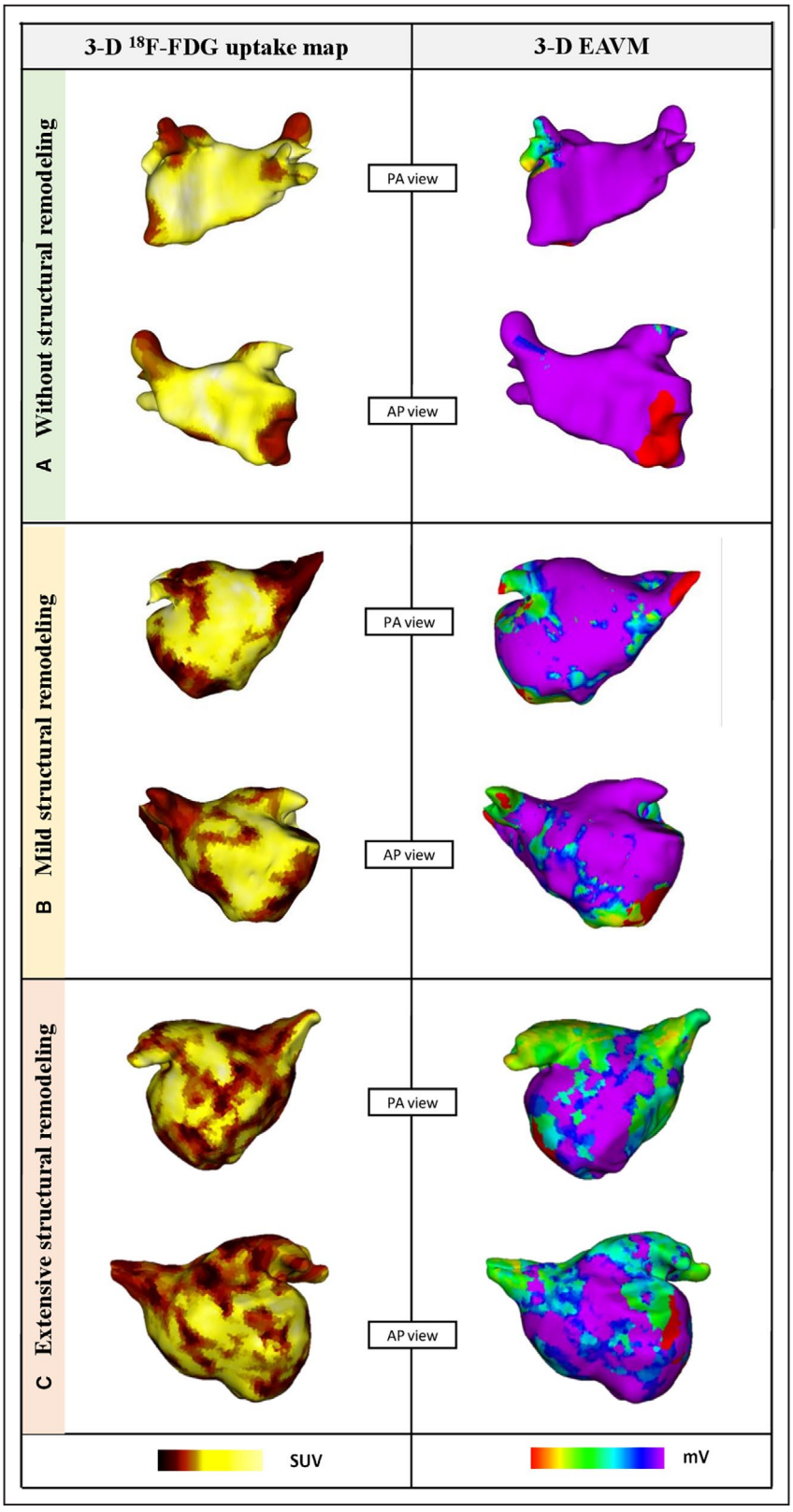

Figures S1 through S3. PVI was successfully executed in all patients with no discernible variation in the ablation strategy, encompassing box isolation, other lines, and complex fractionated atrial electrograms, between patients with low or extensive LGU. No complications such as cardiac perforation, systemic embolism or stroke, atrial-esophageal fistula, pulmonary stenosis, or mortality were encountered during the procedure.

Correlations Analysis Between the Extent of LVA, LGU, LGE and LAVI

Figure 2 depicts 3 examples of coregistered segmented 3D ^{18}F-FDG LGU maps with 3D EAVM LVA acquired during AF. In Figure 2A, a patient is illustrated without detectable LGU area and no LVA extent. Figure 2B displays a patient with a mild LGU extent (accompanied by corresponding LVA) in the posterior and inferior segments of the left atrium around the ostia of the left inferior PV and right inferior PV, as well as in the anteroseptal part of the LA. Figure 2C presents an instance of extensive LGU and LVA, where the tracer distribution's heterogeneity is more pronounced. Significant LGU extent is observed in the LA's posterior and inferior parts, along with the anterior and anteroseptal parts, corresponding to abnormal atrial tissue with LVAs in the equivalent regions. Quantitative analysis of this relationship confirmed a good correlation of R^2=0.54 (P<0.001) between global LGU and LVA extent (Figure 3A) as well with segmental LGU and LVA extent (Figure 4). Additionally, a good correlation was observed between mean voltage and SUV (R^2=0.42, P<0.001) (Figure 3B). LAVI showed a weak but significant correlation with LVA extent (P=0.039, R^2=0.20) and no correlation with global LGU extent (R^2=0.01, P=0.58). Finally, atrial fibrosis evaluated with LGE CMR did not correlate with either the extent of LVA (P=0.62, R^2=0.01) nor with global LGU (P=0.52, R^2=0.01).

Predictive Value of Noninvasive Imaging Modalities

The receiver operating characteristic curves for the prediction of moderate or important global LVA extent during the ablation procedure for the different noninvasive imaging parameters are shown in Figure 5. LGU had the highest AUC (0.78 [95% CI, 0.58–0.97]). This was significantly higher (P=0.03) than the AUC for LGE (AUC, 0.55 [95% CI, 0.32–0.79]) and LAVI demonstrated moderate discriminating value (AUC, 0.63 [95% CI, 0.43–0.83]). After adjusting for age, estimated glomerular filtration rate, CHA_2DSVAS_2C score, LAVI, E/e′, LA stiffness, LGU extent, LA SUV, and LGE extent, global LGU emerged as the best predictor of elevated LVA extent (coefficient point estimate of 4.46, P<0.001) (Table 3). Similar results were observed during right atrial pacing (Data S2).

Follow-Up and AF Recurrence Outcome

After the CA procedure, 25 patients (69%) were treated with beta blockers, 4 patients (11%) with sotalol, 6 patients (17%) with amiodarone, and 6 patients (17%) with class I antiarrhythmic drugs. A documented recurrence of AF lasting longer than 30 seconds after the initial ablation procedure, with or without the use of antiarrhythmic medications, occurred in 18 patients (50%). Patients with recurrent atrial tachyarrhythmias were older (66.5±8.7 versus 62.4±8.3 years, P=0.090), more often had hypertension (46.7% versus 31.6%, P=0.195), and had a higher CHA_2DS_2-VASc score but, none of the clinical parameters or antiarrhythmic drug treatment administered after CA procedure showed a statistically significant difference between patients with and without AF recurrence. Clinical parameters and noninvasive imaging modalities predictors of arrythmia recurrence are shown in Table 4. Univariable predictors of AF recurrence were LAVI and global LGU extent >17%. In multivariable regression analysis, high LGU extent remained the only independent predictors of recurrent atrial

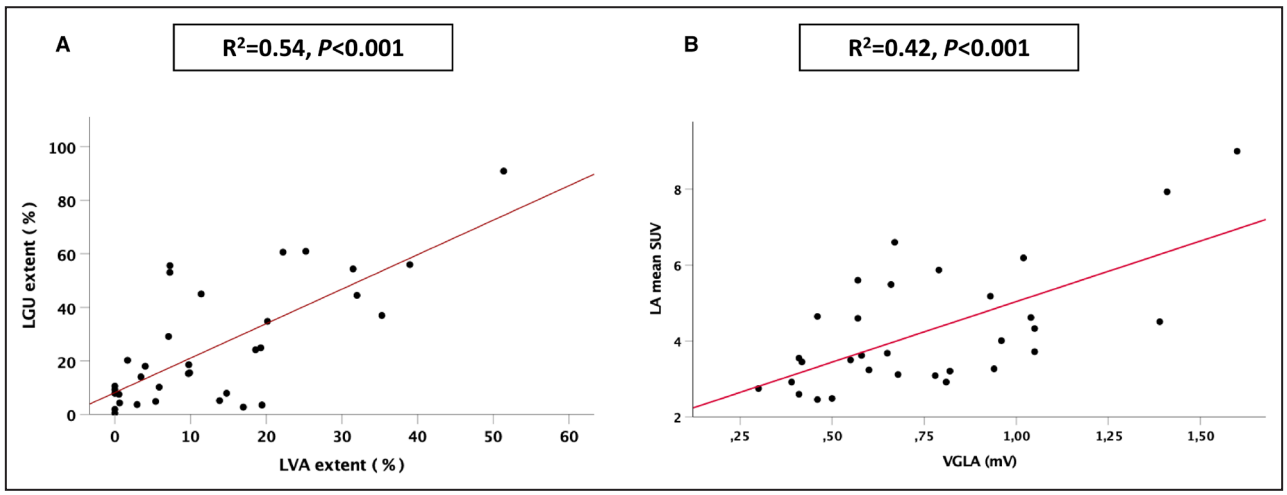

Figure 3. Correlation between the different imaging modalities evaluated through linear regression analysis and the Pearson correlation coefficient.

A, Correlation between LGU extent (with ^{18}F-FDG-PET) and LVA extent (with EAVM). **B**, Correlation between LA mean SUV (with ^{18}F-FDG-PET) and VGLA (with EAVM). LA indicates left atrium; LGU, low glucose uptake; LVA, low voltage area with electroanatomical voltage map acquired in atrial fibrillation; SUV, standardized uptake value; and V_{GLA}, global left atrial voltage acquired in atrial fibrillation.

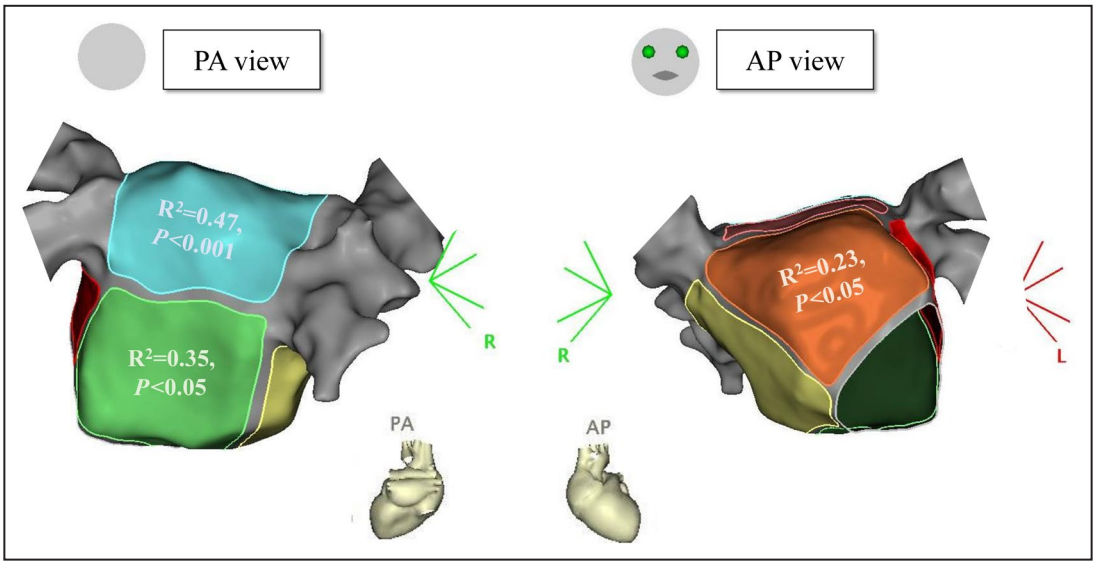

Figure 4. Illustration of the LA segmentation with PA and AP view.
The posterior segment is marked in blue, the inferior in green and the anterior in orange. The result of the correlation between LGU and LVA evaluated through linear regression analysis and the Pearson correlation coefficient are reported in the corresponding segments. AP indicates anteroposterior view; LA, left atrium; LGU, low glucose uptake; LVA, low voltage area with electroanatomical voltage map acquired during atrial fibrillation; and PA, posteroanterior view.

tachyarrhythmias following CA procedures (P<0.001). Receiver operating characteristic curves analysis for the prediction of AF recurrence after the CA are shown in Figure 6, and Kaplan–Meier curves for estimation of freedom from documented atrial fibrillation according to the 2 LGU extent groups are shown in Figure 7. LVA extent had the highest AUC (0.74, [95% CI, 0.56–0.92]) to predict AF recurrence, surpassing LGE (AUC, 0.55 [95% CI, 0.33–0.76]). global LA voltage had also a good predictive value with AUC, 0.67 (95% CI, 0.48–0.87). Among the noninvasive imaging tools, LAVI and LGU extent demonstrated the best predictive accuracy to predict AF recurrence (AUC, 0.71 [95% CI, 0.53–0.89] and 0.67 [95% CI, 0.48–0.86], respectively). AF recurrence-free survival rates were respectively 77% in patients with low LGU extent and 35% in patients with moderate or important global LGU extent (log-rank, P=0.026).

DISCUSSION

The principal findings of the present study can be summarized as follows:

1. A 3D quantitative map of LGU extent with ^{18}F-FDG PET showed a good correlation with LVA extent.
2. Among the noninvasive modalities, LGU evaluated with ^{18}F-FDG PET in the atrial walls had the highest diagnostic accuracy for predicting LVA extent.
3. LGU extent quantification with 3D ^{18}F-FDG PET map independently allowed prediction of the success of CA procedure in patients with peAF.

PVI is now widely accepted as the cornerstone of AF ablation and is recommended during all CA procedures.[1–3] Nevertheless, the notable recurrence rates observed in patients with persistent and long-standing persistent AF following PVI alone have prompted ongoing efforts to identify supplementary strategies to enhance the outcomes of AF ablation.[4,5] Therefore, in patients with peAF, the identification and the assessment of the LA cardiomyopathy substrate have gained clinical significance. The evolving trend in ablation strategy is increasingly tailored, relying on the treatment of fibrotic areas discerned through various imaging technologies to ameliorate the underlying substrate of arrhythmia.[9–12]

In our study we used 3D EAVM combining anatomical and electrical information by catheter sequential point-by-point or simultaneous multielectrode mapping, as reference standard to identify atrial fibrosis. Indeed, EAVM facilitates the identification of LVA, voltage reduction, slowed conduction, and complex fractionated signals—manifestations indicative of structural changes and the hallmark of fibrosis.[23] Studies have shown that patients with peAF have a higher extent of LVAs than those with paroxysmal AF. Notably, the extent of LVAs has been identified as an independent predictor for recurrence events following AF ablation procedures.[24] Furthermore, these LVAs can be directly targeted with radiofrequency ablation

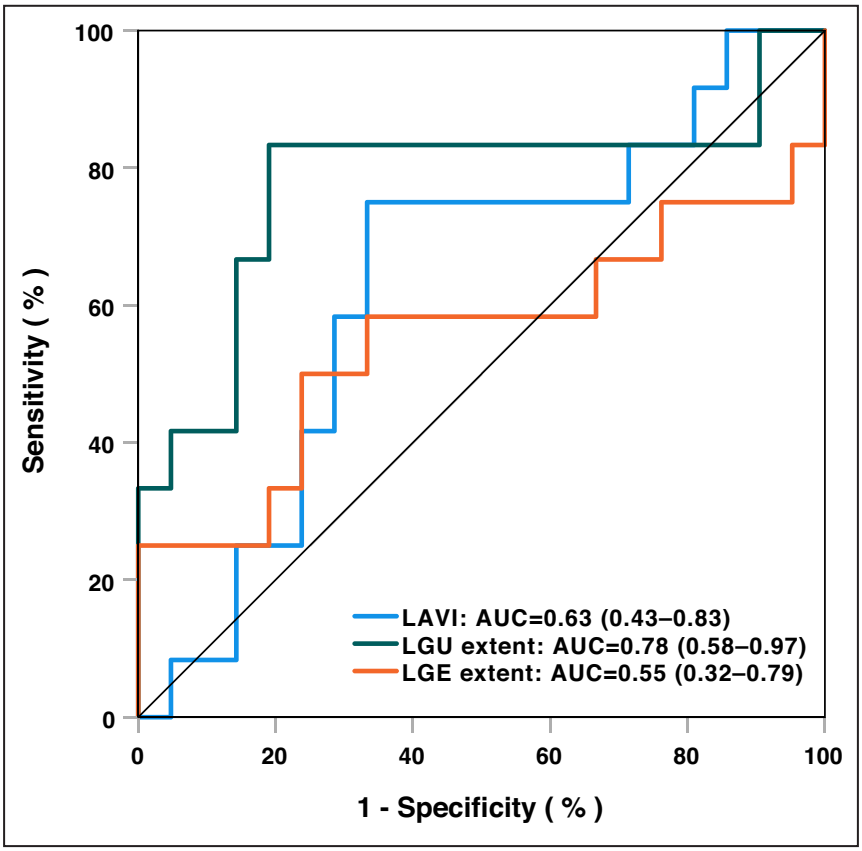

Figure 5. Receiver-operating characteristic curve analysis for prediction of moderate or extensive LVA during EAVM.
AUC indicates area under the curve; EAVM, electroanatomical voltage mapping; LAVI, left atrium volume index; LGE, extent fibrosis detected with late gadolinium enhancement cardiac magnetic resonance imaging; LGU, low glucose uptake; and LVA, low voltage area.

to perform substrate modification. These tailored and therapeutic approaches targeting atrial fibrosis have been reported to improve ablation success rates in patients with peAF.[9–11] However, EAVM with LVA is an invasive method available only at the time of ablation and is not of value for selecting CA candidates before the procedure.

In the present study, we conducted a comprehensive multimodal comparison of FDG-PET LGU with other established markers of atrial structural

Table 3. Multivariable Linear Model for the Prediction of LVA

	Univariable analysis		Multivariable model	
	Coefficient (95% CI)	*P* value	Coefficient (95% CI)	*P* value
Age	0.39 (−0.18 to 0.92)	0.133		
Estimated glomerular filtration rate	−0.14 (−0.39 to 0.09)	0.226		
CHA_2DSVAS_2C	0.42 (5.45 to 20.04)	0.789		
LA volume indexed	0.20 (−0.04 to 0.45)	0.094	1.74 (−0.25 to 0.31)	0.092
E/e′	2.05 (1.08 to 3.03)	<0.001*	3.08 (0.42 to 2.01)	0.005*
LA stiffness	11.51 (6.78 to 16.27)	<0.001*		
Global LGU extent	0.41 (0.27 to 0.55)	<0.001*	4.46 (0.17 to 2.01)	<0.001*
LA standardized uptake value	−3.82 (−6.54 to -1.10)	0.007*		
Late gadolinium enhancement fibrosis	0.12 (−0.37 to 0.62)	0.623		

Regression coefficients are presented as value (95% CI). LA indicates left atrium; LGU, low glucose uptake; and LVA, low voltage area.
*Indicate *P* value <0.01.

Table 4. Cox Univariable and Multivariable Predictors for Prediction of Recurrent Arrhythmia

	Univariable analysis		Multivariable model	
	Coefficient (95% CI)	*P* value	Coefficient (95% CI)	*P* value
Age	1.06 (0.97– 1.16)	0.177		
Estimated glomerular filtration rate	1.02 (0.97– 1.06)	0.383		
CHA_2DSVAS_2C	1.48 (0.89– 2.46)	0.136		
LA volume indexed	1.05 (1.01– 1.10)	0.044	1.05 (0.99– 1.10)	0.067
E/e′	1.14 (0.91– 1.42)	0.249		
LA stiffness	1.39 (0.53– 3.62)	0.501		
LA standardized uptake value	0.81 (0.49– 1.32)	0.385		
Global LGU extent	1.02 (0.99– 1.05)	0.303		
LGU extent>17%	5.96 (1.33– 26.66)	0.020	5.72 (1.14– 28.58)	0.034
Late gadolinium enhancement fibrosis	1.01 (0.94– 1.09)	0.719		

Regression coefficients are presented as value (95% CI). LA indicates left atrium; and LGU, low glucose uptake.

remodeling. As previously described, LA size by echocardiography emerged as a pertinent factor associated with the procedural outcome of AF and demonstrates correlation with atrial fibrosis.[2,14] However, its utility is constrained by low sensitivity, as it may overlook small amounts of fibrosis. Our study unveiled a significant albeit modest correlation between LAVI and LVA extent, a moderate correlation with LGU, and a stronger predictive association with the success rate of the procedure. Remarkably, most echocardiographic

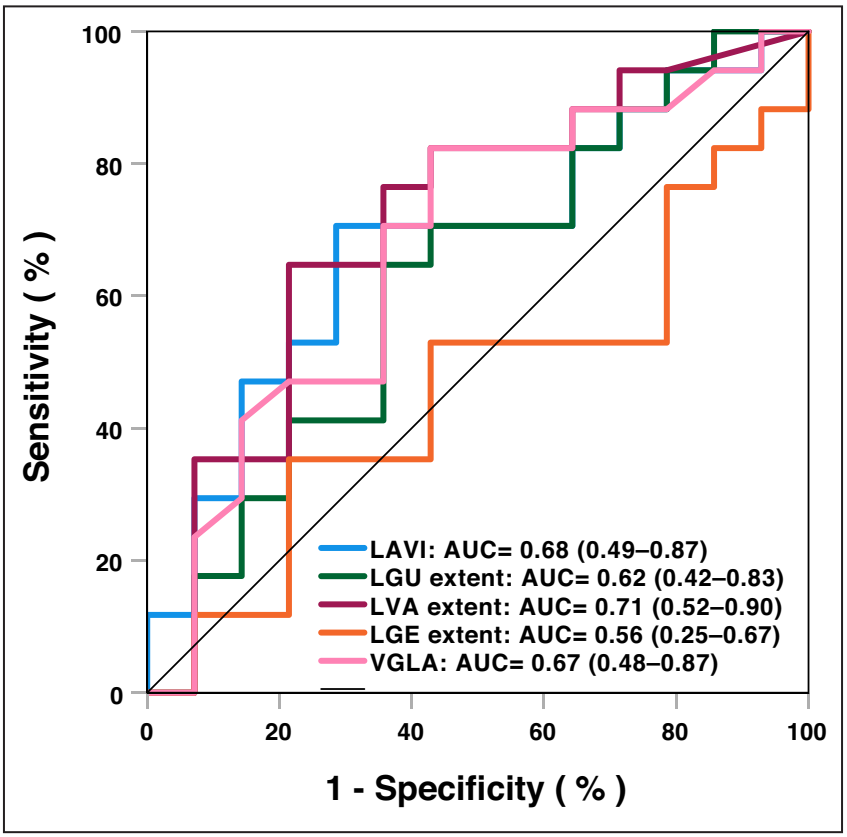

Figure 6. Receiver-operating characteristic curve analysis for prediction of atrial fibrillation recurrence after catheter ablation.
AUC indicates area under the curve; LAVI, left atrium volume index; LGE extent, fibrosis detected with late gadolinium enhancement cardiac magnetic resonance imaging; LGU, low glucose uptake; LVA, low voltage area; and V_{GLA}, global left atrial voltage acquired in atrial fibrillation.

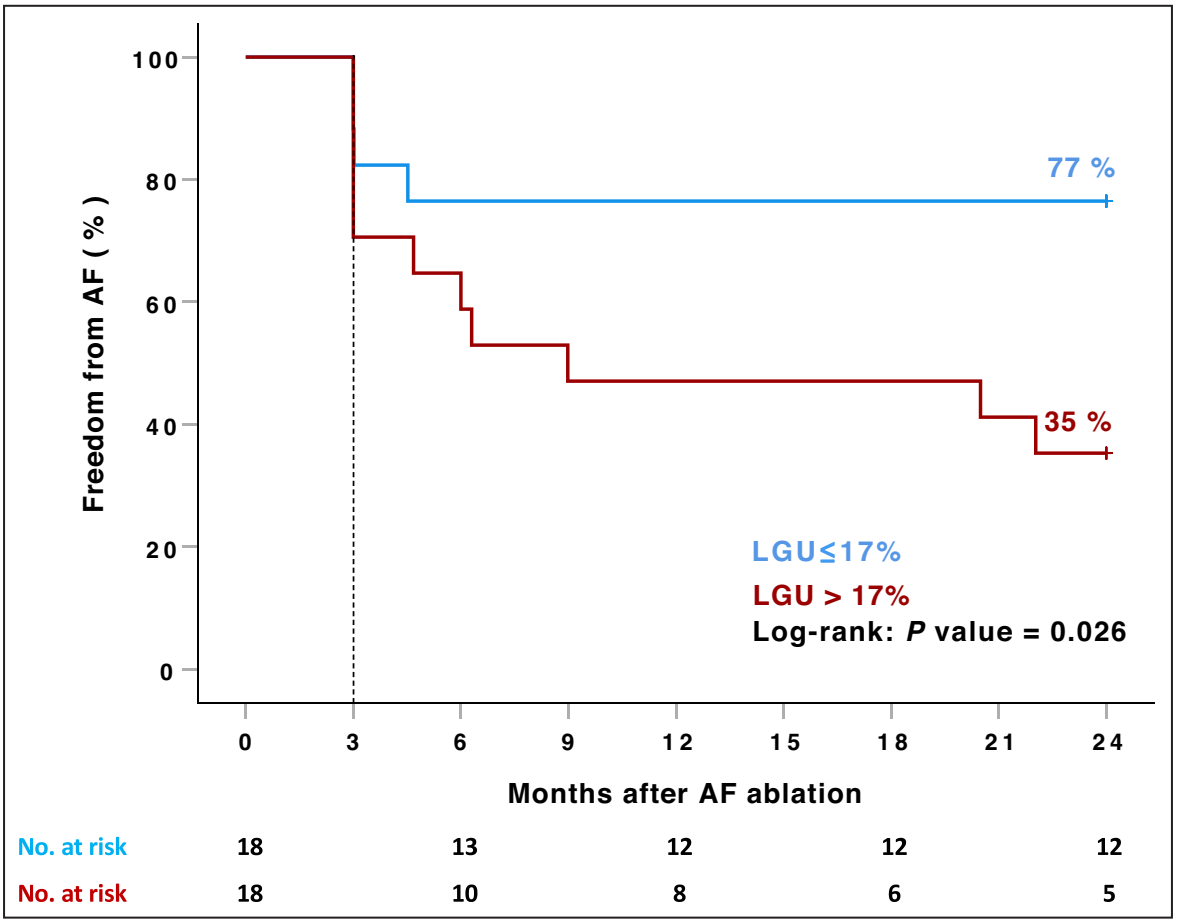

Figure 7. Kaplan–Meier estimates of freedom from documented atrial fibrillation more than 30 seconds after AF ablation procedure according to LGU extent, with or without the use of antiarrhythmic medications.
AF indicates atrial fibrillation; and LGU, low glucose uptake.

parameters linked to atrial remodeling exhibited significantly elevated values in the cohort of patients displaying a considerable extent of LGU. This underscores the relevance of incorporating additional echocardiographic parameters such as LAVI obtained through 3D transthoracic echocardiography, as well as metrics assessing atrial stiffness, LA asynchrony, and LA contractile dysfunction through speckle tracking echocardiography and longitudinal strain. These parameters provide valuable insights into the evaluation of LA structural remodeling and atrial cardiomyopathy.[14]

We also performed a comprehensive cross-comparison of ^{18}F-FDG LGU and LVA to CMR-LGE, which has been advocated as a noninvasive imaging method for identifying atrial fibrosis.[16] The DECAAF study proposed a scoring system (Utah score) for the area of delayed enhancement, the extent of fibrosis evaluated by LGE CMR predicting the outcome of AF ablation and suggesting that CMR quantification of fibrosis may play a role in the appropriate selection of patients most likely to benefit from AF ablation.[17] Some studies have shown a good correlation between LGE-CMR and LVA extent with EAVM.[16,17] However, in our present work, LGU did not correlate well LGE CMR, but LGE-CMR did also not correlate well with LVA-EAVM nor predict outcomes. This is accordance with other works which found disappointing correspondence between LGE-CMR and EAVM.[18,19] Potential explications may be the difficulties of the acquisition process, particularly during arrhythmia,[18,19] and the variability in specialized postimaging processing and threshold to differentiate normal from fibrotic tissue among different studies.[25–28] In our study we used an identical protocol as the DECAAF study and tested several reported methods for LGE quantification; however, we did not find superior results with any method, as detailed in Figure S4. Finally, the value of LGE-CMR has recently been questioned by the negative results of the DECAAF II trial, which could not find added value in AF recurrence with an LGE-CMR-guided ablation strategy.[20]

The novelty of our study lies in proposing nicotinic acid stimulated ^{18}F-FDG PET in order to identify atrial fibrosis in atrial cardiomyopathy. Indeed, AF is

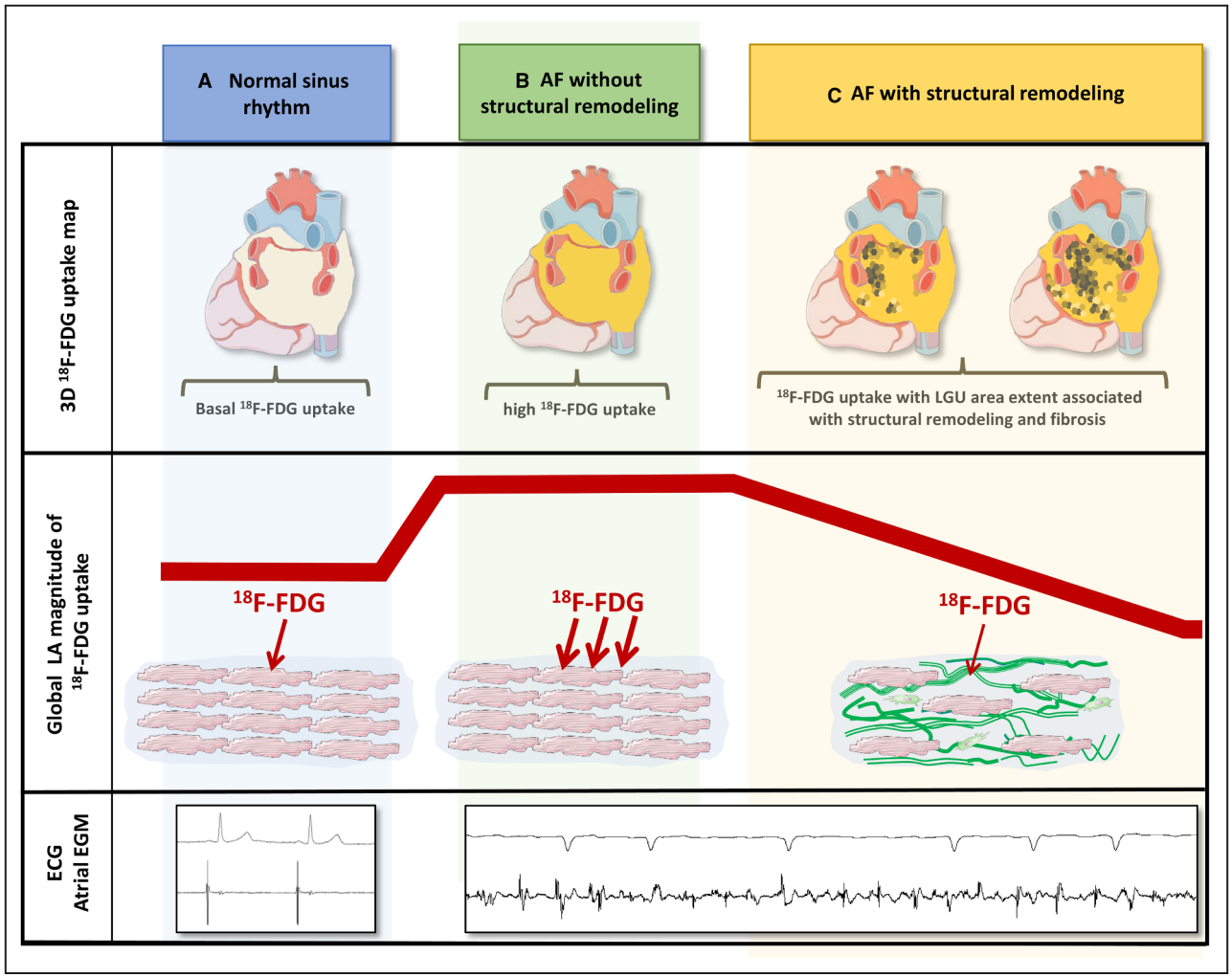

Figure 8. Schematic diagram of FDG uptake interpretation.
A (blue), illustration of patient in SR with normal LA wall ^{18}F-FDG uptake in PA views. **B** (green), patient during AF without structural remodeling and showing homogenous distribution of the tracer with increased LA wall ^{18}F-FDG uptake. **C** (yellow), patient during AF with structural remodeling and showing heterogenous distribution of the tracer with variable magnitude of LA wall ^{18}F-FDG uptake. After administration of a nicotinic acid derivative (acipimox), compared with SR, the LA behaves similarly to the hibernating LV, significantly enhancing atrial ^{18}F-FDG uptake during persistent AF (blue to green). In case of viable atrial myocytes ^{18}F-FDG uptake is thus increased.[21] In patients with LA structural remodeling (yellow), LA FDG-PET 3D map illustration shows heterogeneous distribution of the tracer in the LA with low FDG uptake areas and variable magnitude of the global LA wall ^{18}F-FDG uptake. These areas of metabolic defects and LGU correlate to areas with low endocardial voltage area suggesting the replacement of myocytes by atrial fibrosis. ^{18}F-FDG indicates ^{18}F-fluorodeoxyglucose; 3D, 3-dimensional; AF, atrial fibrillation; EGM, electrogram; LA, left atrium; LGU, low glucose uptake; LV, left ventricle; PA, posteroanterior view; PET, positron emission tomography; and SR, sinus rhythm.

characterized by irregular high-frequency excitation and contraction at the atrial level. As shown previously, atrial cardiomyocyte energy metabolism during AF is associated with metabolic stress and a series of modifications at the cellular level, triggering a metabolic shift to a more fetal phenotype and AMP-activated protein kinase activation.[8,29] These changes increase glucose transporters' expression and promote its trafficking into the sarcolemma, enhancing glucose uptake.[8] Moreover, several retrospective and prospective works, including patients with paroxysmal and peAF, have studied FDG uptake in LA using strategies to suppress physiological myocardial FDG uptake (prolonged fasting, dietary manipulation, or heparin loading). These studies proposed that the FDG uptake was related to the increased activity of atrial structures and epicardial adipose tissue and inversely correlated with LA fibrosis.[30–32] However, the image quality of FDG PET of the LA was poor due to variable uptake and partial volume effect and thin atrial wall. In addition, under such conditions FDG signal may corresponded to the metabolic activity of either the atrial wall, the epicardial adipose tissue, or both.[31] In the TRIATLON (Atrial Perfusion–Metabolism and Fibrosis in Atrial Fibrillation) project, the study population was

homogenous with patients without diabetes with peAF. The protocol details and the FDG uptake interpretation are different and summarized in Figure 8. We demonstrated that after administration of a nicotinic acid derivative (acipimox) (same preparation as used in patients with coronary artery disease to evaluate the myocardial viability) the LA exhibits similar behavior to the hibernating LV, enhancing significantly ^{18}F-FDG uptake during AF.[21,33] Furthermore, we optimized acquisition with sufficient spatial resolution, achieving excellent LA visualization. This permitted us to analyze various structures, including the fossa ovalis, mitral annulus, PV ostia, and LA appendage. The latter allowed us to create a 3D LA uptake map, providing a faithful representation of the LA wall anatomy.[21,33] Therefore, through a detailed analysis of this ^{18}F-FDG PET 3D map, we shown an interesting correlation between PET parameters and many clinical and imaging markers of atrial structural remodeling. This correlation between FDG uptake defects and LVA extent on EAVM, indicated that extent of LGU could represent a new and original marker to highlight LA fibrosis.

Clinical Implications

The present study demonstrated the ability of acipimox enhanced ^{18}F-FDG PET to accurately identify LVA and structural remodeling of the LA in patients with peAF and suggests that this technique might be useful for predicting outcomes of CA. Indeed FDG-PET performed better than LGE-CMR, which suffered from poor image quality and was not accurate to identify LVA. Nicotinic acid enhanced ^{18}F-FDG-PET could thus be a better alternative to LGE-CMR for preoperative assessment of fibrosis before CA in peAF, although the technique has some disadvantages, in particular high cost, and radiation exposure. Nevertheless, if PET CMR allows better identification of CA candidates, these limitations are clearly better than performing CA.

Limitations

This study was conducted at a single center and featured a limited sample size. The clinical insights gained from our investigation warrant validation in larger patient cohorts. Notably, diabetes was an exclusion criterion in our study due to potential interference with FDG uptake. Future studies should explore the utility of PET in patients with diabetes to visualize FDG uptake. It is essential to acknowledge that FDG PET may not exclusively evaluate atrial metabolism; it could also reflect the metabolism of epicardial adipose tissue or inflammatory macrophages. AF induces a hibernating-like phenotype in atrial cardiomyocytes, leading to fibroblast replacement and the development of fibrotic tissues. Although obtaining LA biopsies is imperative to address these complexities, our study's positive correlation between the 3D quantitative analysis of LGU with the ^{18}F-FDG uptake map and the extent of LVA aligns with previous observations,[21,33] indicating that LGU could be associated with atrial electrical scaring in whom fibroblast replaced cardiomyocyte and could predict ablation procedure outcome. Finally, LVA measurements were acquired with CARTO3 and a deflectable 12-pole circular mapping catheter with 25-15 loop diameter, and 8 mm interelectrode spacing. Therefore, our findings might not apply to other mapping systems and catheters.

CONCLUSIONS

Low glucose uptake areas on nicotinic acid enhanced ^{18}F-FDG PET in patients with peAF closely correlated with areas of electrical low voltage area during electroanatomic voltage mapping indicating that LGU detects LA fibrosis. Furthermore, the spatial extent of LGU predicted the success after CA procedure indicating that this parameter can noninvasively evaluate the severity of atrial structural remodeling in atrial cardiomyopathy. These findings support the potential role of ^{18}F-FDG-PET in improving the evaluation and management of patients with peAF candidates for CA procedures.

ARTICLE INFORMATION

Received February 18, 2025; accepted May 13, 2025.

Affiliations

Division of Cardiology, Department of Cardiovascular Diseases, Cliniques Universitaires St. Luc, Pôle de Recherche Cardiovasculaire (CARD), 10 avenue hippocrate, Brussels, 1200, Brussels, Belgium (T.R., B.L.G., Q.G., C.S., V.V., A.W., D.G., E.N., C.B., S.M.); and Pole Molecular Imaging, Radiotherapy & Oncology (MIRO), Institut de Recherche Expérimentale et Clinique (IREC), Université Catholique de Louvain, Brussels, Belgium (M.H., V.R.).

Acknowledgments

The authors wish to thank Constantin Bachtsevanos, Priscila Martinez, Carina Coito Faustino, Thibaut Ruzie, Sotiria Sapuntji, Arthur Vanderbreetstraeten, Sarah Grandi, Valérie Kisters, Marine Falmagne, Isabelle Remy, Catherine Vacquez, Benjamin Pourbaix, Thomas Paulus, Virginie Depoortere, Amal Oulad Bouchetta, and Soundes Bourouis for their help in collecting and analyzing the data presented here.

Sources of Funding

Grant support was provided by the Fonds pour la Chirurgie Cardiaque and by an unrestricted grant by Pfizer and Daiichi Sankyo to the cardiology division. Dr Gerber has received grant support from the Fonds p La Chirurgie Cardiaque de l'Universite Libre de Bruxelles.

Disclosures

None.

Supplemental Material

Data S1
Table S1
Figures S1–S4

REFERENCES

1. Hindricks G, Potpara T, Dagres N, Arbelo E, Bax JJ, Blomström-Lundqvist C, Boriani G, Castella M, Dan GA, Dilaveris PE, et al. 2020

ESC guidelines for the diagnosis and management of atrial fibrillation developed in collaboration with the European Association for Cardio-Thoracic Surgery (EACTS): the task force for the diagnosis and management of atrial fibrillation of the European Society of Cardiology (ESC) developed with the special contribution of the European Heart Rhythm Association (EHRA) of the ESC. *Eur Heart J*. 2021;42:373–498. doi: 10.1093/eurheartj/ehaa612

2. Tzeis S, Gerstenfeld EP, Kalman J, Saad EB, Sepehri Shamloo A, Andrade JG, Barbhaiya CR, Baykaner T, Boveda S, Calkins H, et al. 2024 European heart rhythm association/Heart Rhythm Society/Asia Pacific Heart Rhythm Society/Latin American Heart Rhythm Society expert consensus statement on catheter and surgical ablation of atrial fibrillation. *Heart Rhythm*. 2024;21:e31–e149. doi: 10.1016/j.hrthm.2024.03.017.
3. Tilz RR, Heeger CH, Wick A, Saguner AM, Metzner A, Rillig A, Wohlmuth P, Reissmann B, Lemeš C, Maurer T, et al. Ten-year clinical outcome after circumferential pulmonary vein isolation utilizing the Hamburg approach in patients with symptomatic drug-refractory paroxysmal atrial fibrillation. *Circ Arrhythm Electrophysiol*. 2018;11:11. doi: 10.1161/CIRCEP.117.005250
4. Verma A, Jiang CY, Betts TR, Chen J, Deisenhofer I, Mantovan R, Macle L, Morillo CA, Haverkamp W, Weerasooriya R, et al. Approaches to catheter ablation for persistent atrial fibrillation. *N Engl J Med*. 2015;372:1812–1822. doi: 10.1056/NEJMoa1408288
5. Brooks S, Metzner A, Wohlmuth P, Lin T, Wissner E, Tilz R, Rillig A, Mathew S, Saguner A, Heeger C, et al. Insights into ablation of persistent atrial fibrillation: lessons from 6-year clinical outcomes. *J Cardiovasc Electrophysiol*. 2018;29:257–263. doi: 10.1111/jce.13401
6. Nattel S, Heijman J, Zhou L, Dobrev D. Molecular basis of atrial fibrillation pathophysiology and therapy: a translational perspective. *Circ Res*. 2020;127:51–72. doi: 10.1161/CIRCRESAHA.120.316363
7. Nattel S, Burstein B, Dobrev D. Atrial remodeling and atrial fibrillation: mechanisms and implications. *Circ Arrhythm Electrophysiol*. 2008;1:62–73. doi: 10.1161/CIRCEP.107.754564
8. Harada M, Melka J, Sobue Y, Nattel S. Metabolic considerations in atrial fibrillation- mechanistic insights and therapeutic opportunities. *Circ J*. 2017;81:1749–1757. doi: 10.1253/circj.CJ-17-1058
9. Huo Y, Gaspar T, Schönbauer R, Wójcik M, Fiedler L, Roithinger FX, Martinek M, Pürerfellner H, Kirstein B, Richter U, et al. Low-voltage myocardium-guided ablation trial of persistent atrial fibrillation. *NEJM Evid*. 2022;1:EVIDoa2200141. doi: 10.1056/EVIDoa2200141
10. Kircher S, Arya A, Altmann D, Rolf S, Bollmann A, Sommer P, Dagres N, Richter S, Breithardt OA, Dinov B, et al. Individually tailored vs. standardized substrate modification during radiofrequency catheter ablation for atrial fibrillation: a randomized study. *Europace*. 2018;20:1766–1775. doi: 10.1093/europace/eux310
11. Sim I, Bishop M, O'Neill M, Williams SE. Left atrial voltage mapping: defining and targeting the atrial fibrillation substrate. *J Interv Card Electrophysiol*. 2019;56:213–227. doi: 10.1007/s10840-019-00537-8
12. Shen MJ, Arora R, Jalife J. Atrial myopathy. *JACC Basic Transl Sci*. 2019;4:640–654. doi: 10.1016/j.jacbts.2019.05.005
13. Yasuda R, Murata M, Roberts R, Tokuda H, Minakata Y, Suzuki K, Tsuruta H, Kimura T, Nishiyama N, Fukumoto K, et al. Left atrial strain is a powerful predictor of atrial fibrillation recurrence after catheter ablation: study of a heterogeneous population with sinus rhythm or atrial fibrillation. *Eur Heart J Cardiovasc Imaging*. 2015;16:1008–1014. doi: 10.1093/ehjci/jev028
14. Marchandise S, Garnir Q, Scavée C, Varnavas V, Le Polain Waroux JB, Wauters A, Beauloye C, Roelants V, Gerber BL. Prediction of left atrial fibrosis and success of catheter ablation by speckle tracking echocardiography in patients imaged in persistent atrial fibrillation. *Front Cardiovasc Med*. 2022;9:856796. doi: 10.3389/fcvm.2022.856796.
15. Tore D, Faletti R, Biondo A, Carisio A, Giorgino F, Landolfi I, Rocco K, Salto S, Santonocito A, Ullo F, et al. Role of cardiovascular magnetic resonance in the management of atrial fibrillation: a review. *J Imaging*. 2022;8:300. doi: 10.3390/jimaging8110300
16. Oakes RS, Badger TJ, Kholmovski EG, Akoum N, Burgon NS, Fish EN, Blauer JJ, Rao SN, DiBella EV, Segerson NM, et al. Detection and quantification of left atrial structural remodeling with delayed-enhancement magnetic resonance imaging in patients with atrial fibrillation. *Circulation*. 2009;119:1758–1767. doi: 10.1161/CIRCULATIONAHA.108.811877
17. Marrouche NF, Wilber D, Hindricks G, Jais P, Akoum N, Marchlinski F, Kholmovski E, Burgon N, Hu N, Mont L, et al. Association of atrial tissue fibrosis identified by delayed enhancement MRI and atrial fibrillation catheter ablation: the DECAAF study. *JAMA*. 2014;311:498–506. doi: 10.1001/jama.2014.3
18. Sramko M, Peichl P, Wichterle D, Tintera J, Weichet J, Maxian R, Pasnisinova S, Kockova R, Kautzner J. Clinical value of assessment of left atrial late gadolinium enhancement in patients undergoing ablation of atrial fibrillation. *Int J Cardiol*. 2015;179:351–357. doi: 10.1016/j.ijcard.2014.11.072
19. Chen J, Arentz T, Cochet H, Müller-Edenborn B, Kim S, Moreno-Weidmann Z, Minners J, Kohl P, Lehrmann H, Allgeier J, et al. Extent and spatial distribution of left atrial arrhythmogenic sites, late gadolinium enhancement at magnetic resonance imaging, and low-voltage areas in patients with persistent atrial fibrillation: comparison of imaging vs. electrical parameters of fibrosis and arrhythmogenesis. *Europace*. 2019;21:1484–1493. doi: 10.1093/europace/euz159
20. Marrouche NF, Wazni O, McGann C, Greene T, Dean JM, Dagher L, Kholmovski E, Mansour M, Marchlinski F, Wilber D, et al. Effect of MRI-guided fibrosis ablation vs conventional catheter ablation on atrial arrhythmia recurrence in patients with persistent atrial fibrillation: the DECAAF II randomized clinical trial. *JAMA*. 2022;327:2296–2305. doi: 10.1001/jama.2022.8831
21. Marchandise S, Raoult T, Garnir Q, Scavée C, Varnavas V, Wauters A, Gruson D, Nellessen E, Hesse M, Beauloye C, et al. Left atrial glucose metabolism evaluation by 18F-FDG-PET in persistent atrial fibrillation and in sinus rhythm. *JACC Basic Transl Sci*. 2024;9:459–471. doi: 10.1016/j.jacbts.2023.11.001
22. El Haddad M, Taghji P, Phlips T, Wolf M, Demolder A, Choudhury R, Knecht S, Vandekerckhove Y, Tavernier R, Nakagawa H, et al. Determinants of acute and late pulmonary vein reconnection in contact force-guided pulmonary vein isolation: identifying the weakest link in the ablation chain. *Circ Arrhythm Electrophysiol*. 2017;10:e004867. doi: 10.1161/CIRCEP.116.004867
23. Takahashi Y, Yamaguchi T, Otsubo T, Nakashima K, Shinzato K, Osako R, Shichida S, Kawano Y, Fukui A, Kawaguchi A, et al. Histological validation of atrial structural remodelling in patients with atrial fibrillation. *Eur Heart J*. 2023;44:3339–3353. doi: 10.1093/eurheartj/ehad396
24. Yamaguchi T, Tsuchiya T, Fukui A, Kawano Y, Otsubo T, Takahashi Y, Hirota K, Murotani K, Eshima K, Takahashi N. Impact of the extent of low-voltage zone on outcomes after voltage-based catheter ablation for persistent atrial fibrillation. *J Cardiol*. 2018;72:427–433. doi: 10.1016/j.jjcc.2018.04.010
25. Chubb H, Aziz S, Karim R, Sohns C, Razeghi O, Williams SE, Whitaker J, Harrison J, Chiribiri A, Schaeffter T, et al. Optimization of late gadolinium enhancement cardiovascular magnetic resonance imaging of post-ablation atrial scar: a cross-over study. *J Cardiovasc Magn Reson*. 2018;20:30. doi: 10.1186/s12968-018-0449-8
26. Kamali R, Schroeder J, DiBella E, Steinberg B, Han F, Dosdall DJ, Macleod RS, Ranjan R. Reproducibility of clinical late gadolinium enhancement magnetic resonance imaging in detecting left atrial scar after atrial fibrillation ablation. *J Cardiovasc Electrophysiol*. 2020;31:2824–2832. doi: 10.1111/jce.14743
27. Eichenlaub M, Mueller-Edenborn B, Minners J, Figueras I, Ventura RM, Forcada BR, Colomer AV, Hein M, Ruile P, Lehrmann H, et al. Comparison of various late gadolinium enhancement magnetic resonance imaging methods with high-definition voltage and activation mapping for detection of atrial cardiomyopathy. *Europace*. 2022;24:1102–1111.
28. Khurram IM, Beinart R, Zipunnikov V, Dewire J, Yarmohammadi H, Sasaki T, Spragg DD, Marine JE, Berger RD, Halperin HR, et al. Magnetic resonance image intensity ratio, a normalized measure to enable interpatient comparability of left atrial fibrosis. *Heart Rhythm*. 2014;11:85–92. doi: 10.1016/j.hrthm.2013.10.007
29. Barth AS, Merk S, Arnoldi E, Zwermann L, Kloos P, Gebauer M, Steinmeyer K, Bleich M, Kääb S, Hinterseer M, et al. Reprogramming of the human atrial transcriptome in permanent atrial fibrillation: expression of a ventricular-like genomic signature. *Circ Res*. 2005;96:1022–1029. doi: 10.1161/01.RES.0000165480.82737.33
30. Ghannam M, Yun HJ, Ficaro EP, Ghanbari H, Lazarus JJ, Konerman M, Shah RV, Weinberg R, Corbett JR, Oral H, et al. Multiparametric assessment of left atrial remodeling using ^{18}F-FDG PET/CT cardiac

imaging: a pilot study. *J Nucl Cardiol*. 2020;27:1547–1562. doi: 10.1007/s12350-018-1429-y

31. Xie B, Chen BX, Nanna M, Wu JY, Zhou Y, Shi L, Wang Y, Zeng L, Wang Y, Yang X, et al. 18F-fluorodeoxyglucose positron emission tomography/computed tomography imaging in atrial fibrillation: a pilot prospective study. *Eur Heart J Cardiovasc Imaging*. 2021;23:102–112. doi: 10.1093/ehjci/jeab088
32. Xie B, Chen BX, Wu JY, Liu X, Yang MF. Factors relevant to atrial ^{18}F-fluorodeoxyglucose uptake in atrial fibrillation. *J Nucl Cardiol*. 2020;27:1501–1512. doi: 10.1007/s12350-018-1387-4
33. Hesse M, Marchandise S, Gerber B, Roelants V. Cardiac atrial metabolism quantitative assessment with analog and digital time of flight-PET/computed tomography. *Nucl Med Commun*. 2023;44:646–652. doi: 10.1097/MNM.0000000000001694